Amino Acids (2005) 28: 177–182
DOI 10.1007/s00726-005-0165-1

Amino Acids
Printed in Austria

Calcium accumulation in neurites and cell bodies of rat cerebellar granule cells in culture: effects on $GABA_A$ receptor function

A. Cupello[1], **A. Esposito**[2], **C. Marchetti**[3], **F. Pellistri**[2], and **M. Robello**[2]

[1] Istituto di Bioimmagini e Fisiologia Molecolare, CNR, Sezione di Genova, Genova, Italy
[2] INFM, Dipartimento di Fisica, Università di Genova, Genova, Italy
[3] Istituto di Biofisica, CNR, Genova, Italy

Received July 1, 2004
Accepted August 1, 2004
Published online February 18, 2005;

Summary. Accumulation of calcium in rat cerebellar granule cells in culture was studied by two photon laser scanning microscopy. Depolarizations by high extracellular potassium induced short-lived increases in calcium in both cell bodies and neurites. However, although the increase in neurites subsided completely after the initial peak, in cell bodies there was a persistent plateau until the high potassium stimulus was removed. On the contrary, the calcium signal due to NMDA receptors activation was persistent in both cell bodies and neurites and remained until the agonist was present.

The nature of these calcium signals provides an interpretation key for the effects of NMDA receptors activation on $GABA_A$ receptors. In particular, the persistent calcium increase in neurites may explain the decrease in GABA activated chloride currents which are related to activation of dendritic/synaptic $GABA_A$ receptors.

Keywords: Two photon microscopy – Intracellular calcium – NMDA receptors – $GABA_A$ receptors – Cerebellar granules

Introduction

Two photon excitation fluorescence microscopy presents several advantages over conventional fluorescence microscopy. By use of long wavelength photons as the excitation input to the fluorophores, it excites spatially restricted zones of the sample with the results of a better resolution and a better preservation of the sample. In particular, it uses infrared radiation which penetrates more deeply into the sample due to less scattering. The dependence of two photon absorption on the square of the radiation intensity (density of photons) limits excitation to the focal volume with a reduced photodamage. In the mean time this approach provides optical sectioning equivalent to the one which can be obtained by confocal microscopy, without any loss of fluorescence light due to a pinhole detector (Diaspro and Robello, 2000). By two photon microscopy it is possible to take spatial windows in different regions of neurons and to evaluate topical changes in calcium ion concentrations by optical imaging. This can be done with a very high time resolution and without damaging the cells. In this way optical imaging of $[Ca^{2+}]$ can be achieved in dendrites and even in dendritic spines (Yuste et al., 1999).

In the experiments reported here we studied by two photon fluorescence microscopy the changes in $[Ca^{2+}]$ induced in cell bodies and neurites of cerebellar granule cells in culture by the activation of voltage dependent- and NMDA receptor associated-channels. The results obtained give clues about the mechanism by which previous NMDA receptor activation reduces the activity of dendritic/synaptic $GABA_A$ receptors in cerebellar granules (Robello et al., 1997; Cupello and Robello, 2000).

Materials and methods

Cerebellar granules cultures

Granule cells were prepared from cerebella of 8 day-old Wistar rats according to the procedure described by Levi et al. (1984). Cells were resuspended in basal Eagle's medium with Earle's salt supplemented with 10% fetal calf serum (Gibco Bio-Cult Ltd, U.K.), 25 mM KCl, 2 mM glutamine and 100 μg/ml gentamicine and plated on Poly-L-Lysine coated glass cover-slips placed in 35-mm plastic dishes at a density of 1.8×10^6 per dish, and kept at 37°C in a humified 95% air-5% CO_2 atmosphere. Experiments were performed between days 5 and 12 after plating.

Two photons microscopy visualization of intracellular $[Ca^{2+}]$

$[Ca^{2+}]$i was measured by Oregon Green 488 Bapta-1, a fluorescent indicator, whose fluorescence intensity is increased upon binding Ca^{2+}.

Neurons were incubated in 6 μM of the cell-permeant AM ester form of the dye for 40–45 min at 37°C, then washed several times with standard saline at room temperature. Cultures were transferred to a recording chamber where they were continually perfused with solutions fed by gravity (3 ml/min). The recording chamber was mounted onto the inverted microscope (Eclipse TE300 Nikon Instruments, Florence, Italy) and a 100× oil immersion objective (N.A. 1.3). The laser beam, tuned at 720 nm, was scanned in the sample by the PCM2000 (Nikon) scan-head and the collected light was acquired through a cut-off filter in order to exclude the excitation radiation. The power at the sample varied from 5 to 7 mW. No detectable damage was ever observed with exposure up to three hours. Images were filtered, frame by frame, by a Wiener filter with a 2×2 kernel and then a threshold was applied in order to discriminate the background. Fluorescence intensity variations over time were calculated as $\Delta F/F_0 = (F - F_0)/F_0$, where F was the fluorescence intensity measured after stimulation and F_0 the basal level. Fluorescence intensity is calculated in arbitrary units using a scale of pixel intensity. Involved pixels are those coming only from the part of cell in the region of interest.

Before stimulation, the cells were perfused with the following control solution: 140 mM NaCl, 5.4 mM KCl, 1.8 mM $CaCl_2$, 1.0 mM $MgCl_2$, 10 mM Glucose; 5 mM Hepes, pH 7.4. For the high potassium solution KCl substituted equimolarly for NaCl: 70 mM NaCl, 75 mM KCl, 2.0 mM $CaCl_2$, 1.0 mM $MgCl_2$, 10 mM Glucose, 5 mM Hepes, pH 7.4. In the experiments in which the voltage gated calcium channels (VGCC) were blocked, 50 μM $CdCl_2$ was added to the solutions. In the treatments with NMDA, Mg^{2+} was omitted both in the control and stimulation solutions and 100 μM NMDA + 50 μM glycine were added to the stimulation solution. D-(-)-2-Amino-5-Phosphono-Valeric acid (APV) was added when appropriate at the concentration of 100 μM.

Patch-clamp studies of GABA activated chloride currents

Membrane currents were measured with the standard whole-cell patch-clamp technique, as described previously (Robello et al., 1993). The holding potential was set to −80 mV in all the experiments reported. This was the most suitable condition to record the total chloride current. GABA activated currents were elicited by perfusion of 10 μM GABA at two minutes intervals. Typically the GABA activated chloride currents showed a peak followed by a decrease to a steady state until GABA was removed (Robello et al., 1993).

In the experiments where the effect of previous activation of NMDA receptors was studied, chloride current was first elicited by 10 μM GABA perfusion. One minute after recovery cells were perfused with 100 μM NMDA (plus 10 μM glycine) for at least one minute and then treated with 10 μM GABA plus 100 μM NMDA (plus 10 μM glycine) to avoid a rapid recovery from the NMDA effect.

The basic external solution consisted of (in mM): 137 NaCl, 5.4 KCl, 1.8 $CaCl_2$, 5 HEPES, 10 glucose. The pH was adjusted to 7.4 using NaOH. In some experiments 1 mM $MgCl_2$ was added or 1.8 mM $BaCl_2$ was substituted for 1.8 mM $CaCl_2$. The basic pipette filling solution contained (in mM): 142 KCl, 10 HEPES, 2 EGTA, 4 $MgCl_2$, 3 ATP Disodium Salt. The pH was adjusted to 7.3 by a Trizma base.

The following solutions were used when the effect of voltage-activated calcium channels was compared with the effect of NMDA. Extracellular (in mM): 132 tetraethylammonium chloride, 10 $CaCl_2$, 10 Glucose, 10 HEPES, 4 4-aminopyridine. The pH was adjusted to 7.4 using a Trizma base. Intracellular (in mM): 142 CsCl, 4 $MgCl_2$, 10 HEPES, 2 EGTA, 3 ATP. The pH was adjusted to 7.3 with a Trizma base.

Results

Changes in [Ca^{2+}] in cell bodies and neurites after stimulation by either high potassium or NMDA

In Fig. 1 we show a granule cell incubated with Oregon Green 6 μM and observed using the two photon microscope. The aim of this study was to follow Ca^{2+} dynamics in terms of intracellular [Ca^{2+}] changes. Thus, the signal was acquired using time series made up of windows of different size. The lateral spatial resolution was 250 nm. For recordings from the cell body, the size of the window, or region of interest (ROI), was 256×16 pixels and the frametime was ∼100 ms, whereas when the ROI was on a neurite, in order to analyze a longer portion, the spatial window was larger (256×80 pixels). Figure 2A shows the time course of the fluorescence signal in ROI on the neuronal cell body during perfusion by a depolarizing high K^+ solution. The signal ($I = \Delta F/F_0$, see *Materials*

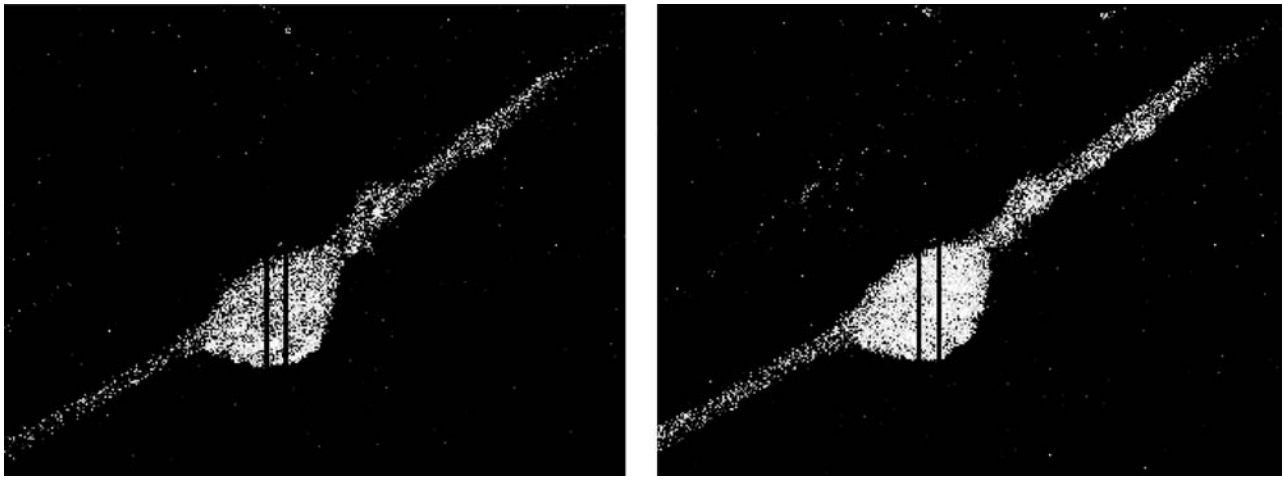

Fig. 1. A granule cell loaded with Oregon Green BAPTA (6 μM) and observed with two photons microscopy before (left) and after (right) stimulation by high K^+

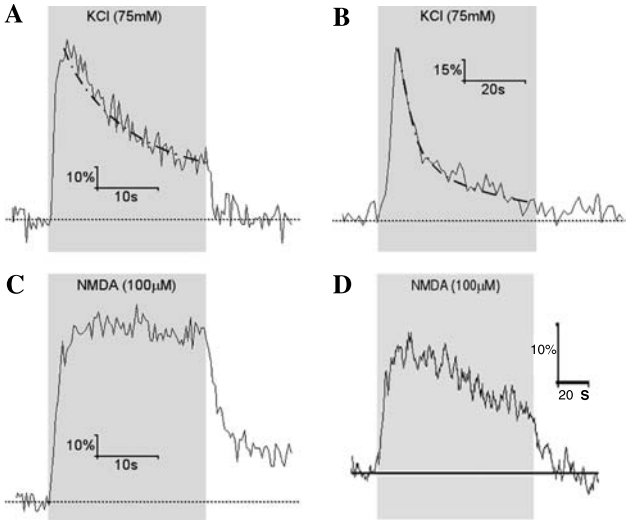

Fig. 2. Cell normalized fluorescence variations during stimulation by depolarizing solution (KCl 75 mM) **A** of a cell body and **B** of a neurite. The dashed line represents the best fit in **A** by a single exponential decaying function with time constant, $\tau = 11$ s and in **B** by a double exponential decaying function with fast and slow time constants equal to 3.5 and 20.5 s respectively. **C** and **D** represent fluorescence variations from, respectively, a cell body **C** and a neurite **D** stimulated by NMDA 100 μM and 50 μM glycine, in 0 Mg^{2+}

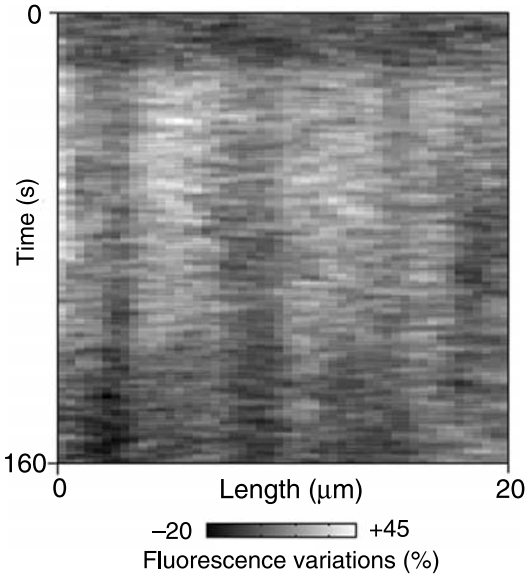

Fig. 3. Different regions along a neurite reacting differently to NMDA 100 μM and 50 μM glycine application in an image of a neurite acquired by two photon microscopy

and methods) was fitted by the exponential expression $I = I_o\, e^{-t/\tau} + I_\infty$. The peak was 65% above baseline, then the signal decayed to a steady state 20% above baseline: τ was 11 s. In 20 cells, the average peak value was $65 \pm 9\%$ (mean $\pm$ SD), the steady state value was $24 \pm 8\%$ and the decay time constant was 9 ± 2 s.

In neurites, perfusion with high potassium always resulted in a sharp peak of fluorescence, followed by decay to the basal level (Fig. 2B). In the case presented, fluorescence rose by 116% and then decayed to the basal level. In 19 neurites, the mean fluorescence increase was $101 \pm 25\%$, significantly different ($p < 0.05$ Student's t test) from that observed in cell bodies. The steady state was close to 0%; the average time constant of fluorescence decay was 2.9 ± 1.5 s. However, in 5 neurites, including the one represented in Fig. 2B, there was also a slow component with a mean time constant of 20 ± 1 s. The time projections analysis showed responses which were quite homogeneous along the neurites (data not shown here).

When neurons were stimulated with 100 μM NMDA (plus 50 μM glycine), in the absence of Mg^{2+}, the cell body fluorescence intensity increased and remained elevated as long as the stimulus was there (Fig. 2C). The time course was quite homogeneous throughout the cell body. The average increase in fluorescence intensity was similar to that obtained with high potassium, with an average increase of $65 \pm 17\%$ ($n = 18$). The cell body responses to NMDA were suppressed by Mg^{2+} (1 mM). Cd^{2+} (50 μM) suppressed the cell body signals elicited by high potassium.

In neurites, the average response to NMDA was smaller than that of the cell body (Fig. 2D): the fluorescence intensity increase being $25 \pm 10\%$ ($n = 9$ neurites). Furthermore, the amplitude of the response, as well as its shape, was discontinuous and varied along the neurite length (Fig. 3). In order to quantify this discontinuity and further characterize the NMDA response, the percentage of ''responsive segments'' along the neurite length was calculated. To do this each neurite window was divided in 50 segments and a segment was considered ''responsive'' when the stimulus (NMDA or high potassium) provoked a fluorescence increase from basal level of at least a standard deviation of the basal signal, calculated from 100 control frames before the stimulus. According to this criterium, $51 \pm 36\%$ of the neurite length was not responsive to NMDA, while only $5 \pm 6\%$ was not responsive to high potassium stimulation: a percentage not significantly different from 0.

GABA induced chloride currents in granule cells and the effect of previous activation of NMDA receptors

The data in Fig. 4B represents the values of the normalized peak chloride currents activated by 10 μM GABA

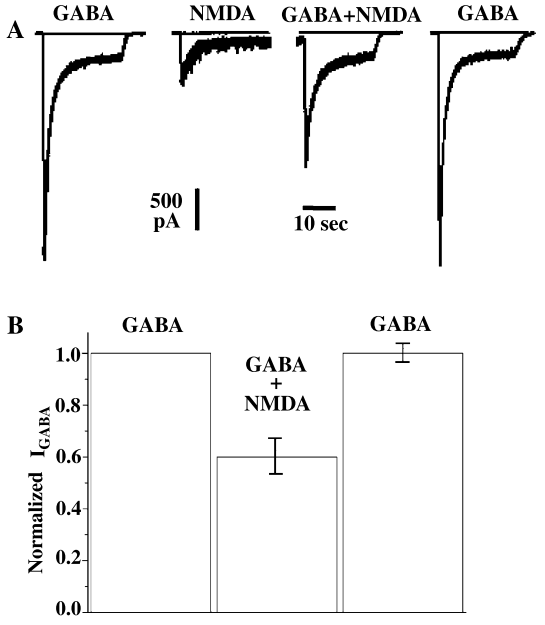

Fig. 4. **A** Effect of NMDA 100 μM plus 50 μM glycine application to cerebellar granules on the chloride current elicited by 10 μM GABA. *From the left*: control chloride current activated by GABA, NMDA activated cationic current, chloride current activated by GABA in the presence of NMDA and finally recovery of GABA activated chloride current after the removal of NMDA. **B** The chloride currents were evaluated (normalized) in reference to that before NMDA application, taken as 1.0

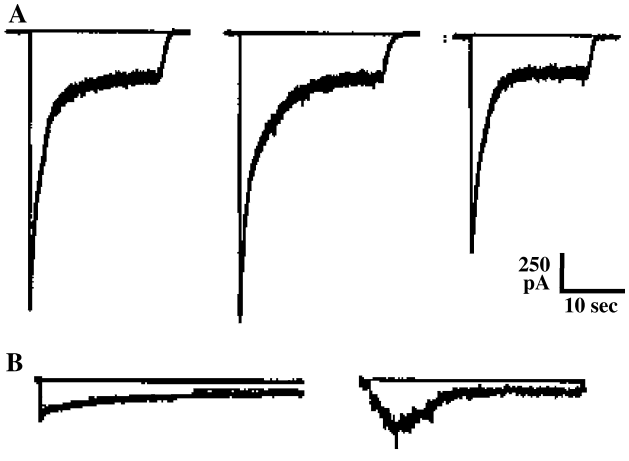

Fig. 5. **A** Profiles of GABA activated chloride currents: control (*left*), after accumulation of Ca^{2+} for 1 min via voltage activated channels (*center*) and after application for 1 min of NMDA 100 μM and 50 μM glycine (*right*). **B** Calcium associated charge accumulation in the two instances of part **A**: *left*, after calcium currents activation by depolarization and *right*, after NMDA receptor activation. From the integral over time of the calcium associated currents, it can be calculated that the charge accumulation in the cell after 1 min is about the double in the case of activation by depolarization (3 nC vs. 1.7 nC)

before and after the application of 100 μM NMDA plus 10 μM glycine, whereas the actual recordings are in Fig. 4A. The results show a 40% reduction in GABA activated current in the presence of NMDA. The effect subsided upon removal of NMDA + glycine.

However, when an even greater amount of Ca^{2+} entered the cells via calcium channels activated by depolarization to +10 mV (voltage gated calcium channels, VGCC) no effect was found on GABA activated peak chloride current (Fig. 5).

No effect was ever found, either due to NMDA or depolarization, on the steady state component of GABA activated chloride current (see Fig. 5).

Discussion

Oregon Green BAPTA-1 is moderately fluorescent in Ca^{2+}-free solution and its fluorescence is enhanced ~14-fold at saturating $[Ca^{2+}]$. Therefore the pattern of fluorescence intensity changes is likely to correlate well with changes in $[Ca^{2+}]_i$. The time course of $[Ca^{2+}]_i$ changes described here for neuronal cell bodies is in good agreement with that reported previously using ratiometric indicators (Ciardo and Meldolesi, 1991; Simpson et al., 1993; Marchetti et al., 1995; Savidge and Bristow, 1997). In neuronal somata, depolarization caused $[Ca^{2+}]_i$ to rise to a peak and then decline to a lower steady state, which was still above baseline. On the contrary, the increase in fluorescence during NMDA treatment was sustained from the beginning to the end, similar to findings reported in a previous study (Simpson et al., 1993). In another study (Ciardo and Meldolesi, 1991), where neurons were stimulated by glutamate instead of NMDA, $[Ca^{2+}]_i$ showed an initial peak, which was suppressed by voltage-gated calcium channel (VGCC) blockers and was absent in subsequent stimulatory treatments. In our experiments, we did not observe such a transient peak that might indicate a contribution of VGCC to the glutamate response. In parallel experiments with conventional microfluorometry and Fura2 (Marchetti et al., 1995; Usai et al., 1999) when neurons were stimulated by glutamate, instead of NMDA, the response was partially antagonized by VGCC blockers, but the effect of the same blockers on the NMDA response was negligible (Marchetti C. and Usai C., unpublished and Usai et al., 1999). Moreover, the calcium response to depolarization was not sensitive to NMDA blockers, including APV and 5-chlorokinurenic acid (Marchetti C., unpublished). Therefore, our experimental results are reminiscent of those reported by Savidge and Bristow (1997): the two responses are independent and the $[Ca^{2+}]_i$ rise stimulated by NMDA is predominantly due to influx through NMDA receptor channels, while depolarization results in Ca^{2+} entry

mainly through VGCCs rather than NMDA receptor channels.

In the cell body, in both stimulating conditions, a sustained plateau was present and Ca^{2+} returned to the basal level only after the stimulus was washed out. Therefore it seems reasonable, as previously suggested (Simpson et al., 1993; Berridge, 1998), that both high K^+ and NMDA treatments trigger release of calcium from intracellular stores, thus providing a substantial and persistent contribution to the $[Ca^{2+}]_i$ in the cell body. The two responses have a significantly different time course, most likely because NMDA channels desensitize more slowly than VGCCs inactivate, resulting in a balance between Ca^{2+} entry, release and sequestration in the case of NMDA, while the sequestration mechanisms predominate during depolarization. The persistent $[Ca^{2+}]$ elevation during NMDA treatment indicates that NMDA channels are not subjected to the calcium-mediated negative feedback mechanism that acts at the synaptic level and restricts the amplitude of calcium transients (Umemiya et al., 2001). This persistent Ca^{2+} elevation may be a significant factor for glutamate-mediated excitotoxicity.

The novelty of our present approach with two-photon microscopy is the possibility of discriminating changes in fluorescence in different regions of the cell, such as neurites, or even small sections of neurites. To our knowledge, this is the first report of $[Ca^{2+}]_i$ measurements in neurites of cerebellar granule cells, although in other neurons Ca^{2+} accumulation has been studied not only in dendrites, but also in dendritic spines (Yuste et al., 1999; Euler et al., 2002). The spatial distribution of VGCC in neurons has been investigated in several studies. Ca imaging and intracellular recording revealed a dominant role of low-threshold T-type calcium channels in mediating Ca influx in dendrites, whereas high-threshold activated VGCC were predominant in the soma both in hippocampal pyramidal cells (Christie et al., 1995) and in neurons of the deep cerebellar nuclei (Gauck et al., 2001). This could also be the case in cerebellar granule cells, because the depolarization stimulated fluorescence signal decayed faster in neurite than in somata, as expected from faster inactivating channels. In addition, in neurites, depolarization driven Ca^{2+} influx is significantly more pronounced than in somata, due to higher surface/volume ratio, but the Ca^{2+} concentration declines rapidly to the basal level during stimulation, without any sustained phase. Thus, differently from cell bodies, calcium-induced calcium-release (CICR) mechanisms appear to be absent in neurites. Finally, the calcium response to depolarization was independent of the position along the process, and there were no insensitive areas, indicating that VGCC are distributed over the whole neuronal surface.

Previous studies indicated that the distribution of ligand gated channels is largely heterogeneous, with obviously a significantly higher density at synaptic sites, where two-photon uncaging of neurotransmitters (Denk, 1994) has been the technique of choice to map the distribution of functional ionotropic receptors (Matsuzaki et al., 2001). A more straightforward calcium imaging approach recently demonstrated the heterogeneous distribution of APV- and CNQX-sensitive channels in primary culture of neocortical neurons and a major role of NMDA receptors in glutamate-driven Ca^{2+} influx (Wang et al., 2002). In cerebellar granule cells, our present data show that, similar to somatic NMDA channels, neurite NMDA channels also desensitize slowly and are not subject to a calcium-mediated negative feedback mechanism, because the time course of fluorescence changes declined slower than the response to depolarization (Fig. 2). Moreover, unlike the response to depolarization, the response to NMDA is significantly weaker (25% increase above baseline) than in cell bodies (65%); whereas in theory the higher surface/volume ratio should contribute to a larger increase of fluorescence, as happens with depolarization. This smaller response suggests that NMDA channel density is lower in neurites than in somata, possibly also as a consequence of uneven distribution along the neurite. In fact, calcium influx in neurites during NMDA treatment occurs in certain segments, but not in others, making it difficult to define a clear ''typical neurite response'' to NMDA. The responsive segments may very well correspond to specific locations of NMDA receptor clusters along the neurite.

The interaction between NMDA receptor activation and subsequent activation of $GABA_A$ receptors is interesting in this context. This is especially so because the peak component of GABA activated chloride current corresponds to dendritic synaptic $GABA_A$ receptors (Robello et al., 1999; Cupello and Robello, 2000). The reduction in this component as a consequence of NMDA receptors activation and calcium influx seems to indicate a proximity between clusters of $GABA_A$ and NMDA receptors. Along this line it is tempting to speculate that along the neurites of the granule cells clusters of the two receptor types alternate, a circumstance which would nicely explain the discontinuity in the regions of calcium accumulation along the neurites (Fig. 3).

In other words clusters of excitatory and inhibitory receptors would reciprocally control each other's activity.

The absence of an effect on $GABA_A$ receptors function by influxes of calcium commanded by direct cell depolar-

ization can be explained by the fact that they take place mostly in the cell bodies. In addition, our present results show that calcium accumulation in neurites following depolarization is short lived. A more sustained signal such as that due to NMDA receptors activation and its spreading to contiguous clusters of $GABA_A$ receptors is evidently needed in order to influence $GABA_A$ receptors function, in the reciprocal control mechanism suggested above.

References

Berridge MJ (1998) Neuronal calcium signaling. Neuron 21: 13–26

Christie BR, Eliot LS, Ito K, Miyakawa H, Johnston D (1995) Different Ca^{2+} channels in soma and dendrites of hippocampal pyramidal neurons mediate spike-induced Ca^{2+} influx. J Neurophysiol 73: 2553–2557

Ciardo A, Meldolesi J (1991) Regulation of intracellular calcium in cerebellar granule neurons: effect of depolarization and of glutamatergic and cholinergic stimulation. J Neurochem 56: 184–191

Cupello A, Robello M (2000) $GABA_A$ receptors modulation in rat cerebellum granule cells. Receptors and Channels 7: 151–171

Denk W (1994) Two-photon scanning photochemical microscopy: mapping ligand-gated ion channel distributions. Proc Natl Acad Sci USA 91: 6629–6633

Diaspro A, Robello M (2000) Two photon excitation of fluorescence for three dimensional optical imaging of biological structures. J Photochem Photobiol 55: 1–8

Euler T, Detwiler PB, Denk W (2002) Directionally selective calcium signals in dendrites of starburst amacrine cells. Nature 418: 845–852

Gauck V, Thomann M, Jaeger D, Borst A (2001) Spatial distribution of low- and high-voltage-activated calcium currents in neurons of the deep cerebellar nuclei. J Neurosci 21: RC158

Levi G, Aloisi F, Ciotti MT, Gallo V (1984) Autoradiographic localization and depolarization induced release of amino acids in differentiating granule cell cultures. Brain Res 290: 77–86

Marchetti C, Amico C, Usai C (1995) Functional characterization of the effect of nimodipine on the calcium current in rat cerebellar granule cells. J Neurophysiol 73: 1169–1180

Matsuzaki M, Ellis-Davies GC, Nemoto T, Miyashita Y, Iino M, Kasai H (2001) Dendritic spine geometry is critical for AMPA receptor expression in hippocampal CA1 pyramidal neurons. Nat Neurosci 4: 1086–1092

Robello M, Amico C, Cupello A (1993) Regulation mechanisms of GABA receptor function in cerebellar granule cells in culture: possible differential involvement of kinase activities. Neurosci 53: 131–138

Robello M, Amico C, Cupello A (1997) A dual mechanism for impairment of $GABA_A$ receptor activity by NMDA receptor activation in rat cerebellum granule cells. Eur Biophys J 25: 181–187

Robello M, Amico C, Cupello A (1999) Evidence of two populations of GABA(A) receptors in cerebellar granule cells in culture: different desensitization kinetics, pharmacology, serine/threonine kinase sensitivity, and localization. Biochem Biophys Res Comm 266: 603–608

Savidge JR, Bristow DR (1997) Routes of NMDA- and K(+)-stimulated calcium entry in rat cerebellar granule cells. Neurosci Lett 229: 109–112

Simpson PB, Challiss RAJ, Nahorski SR (1993) Involvement of intracellular stores in the Ca^{2+} responses to N-methyl-D-aspartate and depolarization in cerebellar granule cells. J Neurochem 61: 760–763

Umemiya M, Chen N, Raymond LA, Murphy TH (2001) A calcium-dependent feedback mechanism participates in shaping single NMDA miniature EPSCs. J Neurosci 21: 1–9

Usai C, Barberis A, Moccagatta L, Marchetti C (1999) Pathways of cadmium influx in mammalian neurons. J Neurochem 72: 2154–2161

Wang G, Ding S, Yunokuchi K (2002) Glutamate-induced increases in intracellular Ca^{2+} in cultured rat neocortical neurons. Neuroreport 13: 1051–1056

Yuste R, Majewska A, Cash SS, Denk W (1999) Mechanisms of calcium influx into hippocampal spines: heterogeneity among spines, coincidence detection by NMDA receptors, and optical quantal analysis. J Neurosci 19: 1976–1987

Authors' address: Dr. Aroldo Cupello, IBFM, CNR, Sezione di Genova, Via De Toni 5, 16132 Genova, Italy,
Fax: 39-010-354180, E-mail: dcupel@neurologia.unige.it